The Meteoritical Society

Meteoritics & Planetary Science 43, Nr 10, 1629–1639 (2008)
Abstract available online at http://meteoritics.org

Non-impact origin of the crater-like structures in the Gilf Kebir area (Egypt): Implications for the geology of eastern Sahara

Letizia ORTI[1], Mario DI MARTINO[2*], Marco MORELLI[1, 3], Corrado CIGOLINI[4], Enrico PANDELI[1], and Alessandra BUZZIGOLI[5]

[1]Dipartimento di Scienze della Terra, Università di Firenze, via La Pira 4, 50121 Firenze, Italy
[2]INAF–Osservatorio Astronomico di Torino, 10025 Pino Torinese, Italy
[3]Fondazione Prato Ricerche, Museo di Scienze Planetarie, via Galcianese 20/H, 59100 Prato, Italy
[4]DSMP, Università di Torino, via Valperga Caluso 35, 10125 Torino, Italy
[5]Laboratorio di Geofisica Applicata, DICeA, Università di Firenze, via S. Marta 3, 50139 Firenze, Italy
[*]Corresponding author. E-mail: dimartino@oato.inaf.it

(Received 1 July 2007; revision accepted 23 April 2008)

Abstract–Several small crater-like structures occur in Gilf Kebir region (SW Egypt). It has been previously suggested that they could be the result of meteoritic impacts. Here we outline the results of our geological and geophysical survey in the area. The proposed impact origin for these structures is not supported by our observations and analyses, and we suggest an alternative interpretation. The crater-like structures in Gilf Kebir area are likely related to endogenic processes typical of hydrothermal vent complexes in volcanic areas which may reflect the emplacement of subvolcanic intrusives.

INTRODUCTION

In the western Egyptian desert, an impressive number of roughly circular, subordinately elliptical structures can be observed; they cover more than 30.000 km^2 on the northeastern side of the Gilf Kebir plateau. They range from a few tens of meters to more than 1 km in diameter. Paillou et al. (2004) suggested that at least 13 of these structures, located between latitudes 23°14′–23°32′ N and longitudes 23°17′– 27°27′ E, could be the result of meteoritic impacts. More recently, Paillou et al. (2006), extended the number of the supposed impact craters to 62. This high number of structures makes their impact origin less plausible.

Also in other regions of the central-eastern Sahara (Libya, Chad, Sudan, and Egypt) several circular structures have been identified from the analysis of satellite images, but only four (Oasis, BP, Aorounga, and Gweni-Fada) have been recognized as impact craters (e.g., French et al. 1974; Koeberl and Reimold 2002; Koeberl et al. 1998, 2005). Five additional structures, the Arkenu double crater (10.3 and 6.8 km in diameter; Paillou et al. 2003), the Kebira crater (about 30 km in diameter; Boston University Press Release 2006) and two more circular structures in northern Chad (8 and 5 km in diameter; González and Alonso 2006) need further in situ investigations.

The present study is an attempt to verify the impact hypothesis for the Gilf Kebir "crater field" by providing new field, petrographical, structural, and geophysical data. These were collected during a recent expedition (November 2005) in the above region reaching the Kebira area as well.

GEOLOGY OF SOUTHWESTERN EGYPT

The investigated area is located east of Gilf Kebir (Fig. 1). It is sandstone plateau located in the south-west corner of Egypt, about 1000 m high (~300 m above the desert floor) and 8000 km^2 wide. In this area the outcropping rocks belongs to the Nubian Sandstones or "Nubia Formation;" this is a term traditionally used in a broad range of stratigraphical and sedimentological connotations to designate a thick series of quartzose sandstones overlying the igneous and metamorphic Archean to Lower Paleozoic basement rocks (Fig. 2a). In particular, the "Nubia Formation" represents the basal beds of the great marine transgression that spread over the most part of Egypt since Cenomanian to Lower Eocene (Klitzsch et al. 1987), and includes continental and neritic deposits. These deposits extend from Dakhla and Kharga oases southwards to Uweinat and further into the Sudan; the thickness of the formation exposed between Jebel Uweinat and Dakhla oasis apparently exceeds 500 m (Klitzsch et al. 1987). In the Jebel

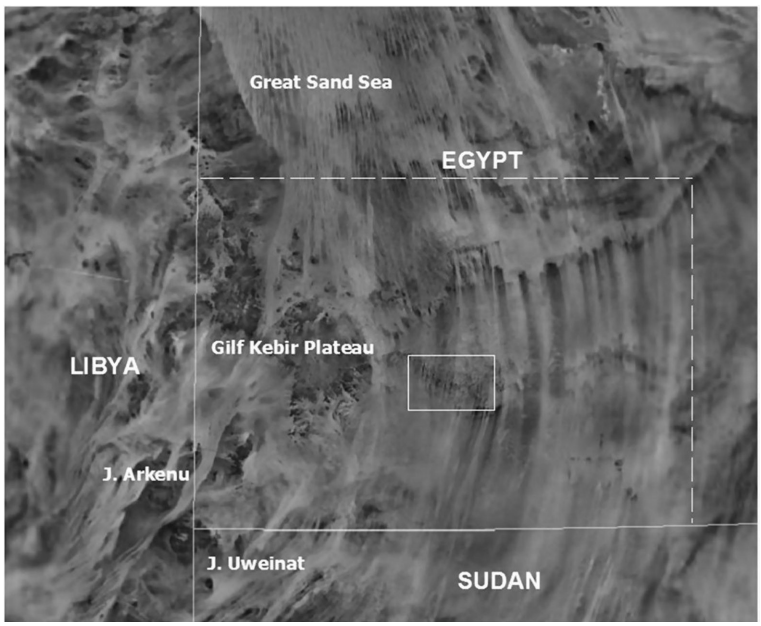

Fig. 1. The southwestern Egyptian desert. The big rectangle (dashed lines together with south and west borders of Egypt) indicate the boundary of Fig. 2a. The small rectangle indicates the investigated area (see Fig. 2b); the latitudes and longitudes are between 23°14′15″–23°34′43″ N and 26°52′10″–27°31′30″ E, respectively (view from Google Earth, see http://www.google.com).

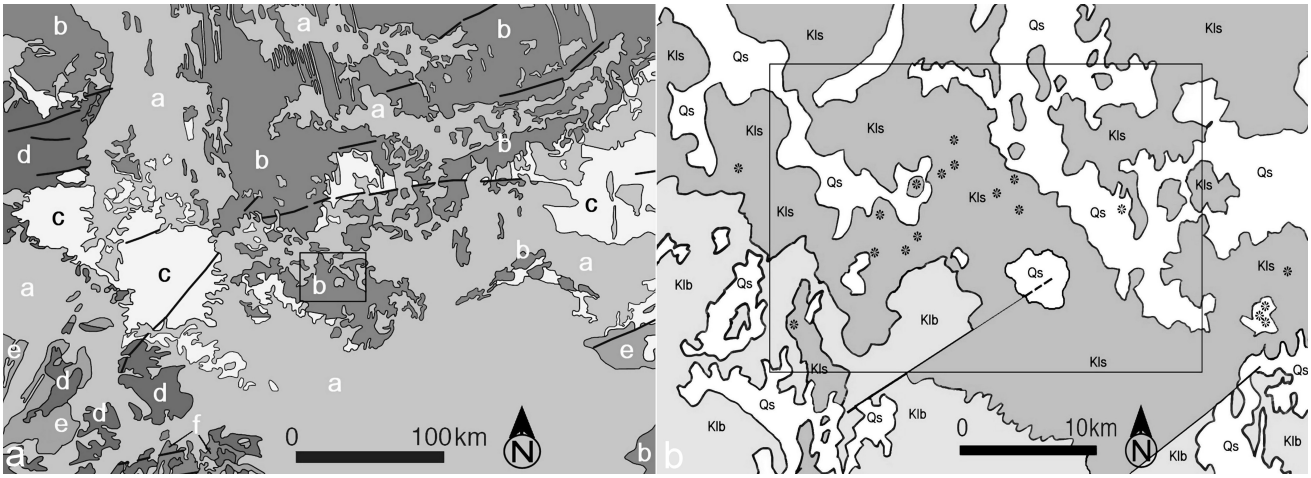

Fig. 2. Geological sketch maps of Gilf Kebir region. The study area is indicated by a rectangle. a) Geological sketch map of southwestern Egypt (Schlüter 2006). a) Sand dunes, sabkhas, cultivated Nile deposits, wadi and playa deposits, beach and corals, calcarenite bars (Quaternary). b) Clastics, phosphate and carbonate rocks (Cretaceous). c) Marine and fluviomarine beds, clastics (Jurassic). d) Mostly clastic rocks (Paleozoic). e) Syn- to post-tectonic granitoids; slightly metamorphosed clastics of the Hammat Group; slightly metamorphosed volcanics of the Dokhah Group; locally gabbros and post-Hammat Group (felsites, porphyries) (Precambrian). f) Mig'if-Hafafit Gneisses and Migmatites (horneblende- and biotite-paragneisses and biotite-gneisses and migmatites) (Precambrian). b) Geological map of investigated area (modified after Klitzsch et al. 1987); the rectangle indicate the boundaries of Fig. 3. Qs: Quaternary sand sheets and dunes. Kls: Sabaya Fm. (Lower-Upper Cretaceous). Klb: Abu Ballas Formation (Lower Cretaceous). ∗: basalts (Paleocene-Eocene).

Uweinat and western Gilf Kebir areas, Devonian-Carboniferous sandstones are locally intercalated between the Nubian Sandstones and the underlying basement rocks (Klitzsch et al. 1987; Said 1990). These represent the northern part of the African shield (or the Saharan Metacraton, according to Abdelsalam et al. [2002]). The basement rocks, mostly exposed in the oasis of Uweinat and in the southern part of the Western Desert (Klitzsch 1987; Abdelsalam et al. 2002), consist of an highly folded metamorphic complex that is intruded by undeformed plutonic masses, forming the relieves of Jebel Uweinat and Jebel Arkenu in Libya. The plutonic rocks are, in turn, cross-cut by aplite and pegmatite dikes (Issawi 1982; Said 1990).

In southern Egypt, lavas and tuffs are interbedded at the base of the Nubian Sandstones. These volcanic rocks, together with some alkaline intrusive bodies cutting the

basement rocks, represent the product of the Upper Cretaceous and the Lower Oligocene magmatic activity (Issawi 1982; Klitzsch et al. 1987). Trachyte and phonolite plugs and cones are also present in this area (particularly south of the Gilf Kebir and north-east of Jebel Uweinat) and represent older volcanics that are associated with the late Paleozoic Hercynian orogenic event.

In southwestern Egypt, the Nubia Formation includes several units. Particularly in the study area they are represented by shallow marine near-shore to coastal siltstones and sandstones, with interbedded alluvial sandstones (Abu Ballas Formation, Lower Cretaceous), and flood-plain sandstones with interbedded channel deposits and paleo-soil horizons (Sabaya Formation, Lower-Upper Cretaceous) (Klitzsch et al. 1987; Said 1990) (Fig. 2b). No specific data about the thickness of the Nubia Formation were defined for the study area, but considering the regional setting of the sandstones (very gently dipping to the North) and the distance of Gilf Kebir region from Uweinat and from Dakhla, it is likely to suppose for this formation a thickness of about 250 m.

All these rocks are covered by Quaternary sand dunes and sheets (Fig. 2b).

THE CIRCULAR STRUCTURES OF EASTERN SAHARA

The eastern Sahara (in particular the Western Desert of Egypt, the eastern side of Libya, the northwestern Sudan and the northern Chad) shows the presence of several circular features with possible distinct origin. The region surrounding the Gilf Kebir Plateau, as well as the top of the plateau itself, is covered by an impressive number of crater-like forms, some of which are associated with Tertiary basalts (Klitzsch 1987). Many of these features have been interpreted as being originated by impact events by Paillou et al. (2004, 2006); among the 62 structures studied by these authors, 10 of these are associated with basalt dikes. Also the area between Jebel Uweinat and Gilf Kebir is covered by many volcanic craters. Some of them have a sandstone rim and are filled with volcanic rocks exhibiting a typical caldera-like structure (e.g., Clayton craters, located about 50 km northeast from Jebel Uweinat; Clayton 1933; Peel 1939; El-Baz 1981), whereas others consist only of volcanic rocks (e.g., at the relief of Jebel Peter and Paul; Dardir 1982). The volcanics generally consist of trachyte and olivine basalts. The trachyte, locally associated with phonolites, rhyolites, and microsyenites, are believed to be related to the Hercynian orogeny that affected the area during the late Paleozoic (El-Baz and Issawi 1982). Some others of these crater-like features, not associated with volcanic rocks, were interpreted as crypto-explosive structures (El-Baz and Issawi 1982). The El-Baz crater (Egypt), located about 320 km east of Kufra, is another circular feature essentially delimited by basaltic dikes intruded into the quartz-arenitic bedrock (El-Baz 1981; Barakat 1994). Also in northern Sudan a group of peculiar circular features of unknown origin, located about 130 km east/southeast of Jebel Uweinat, have been reported (El-Baz and Issawi 1982). In the eastern part of Libya, four craters have been identified: Oasis (about 120 km north/north-east of Kufra), BP (about 80 km north of the Oasis crater), and the Arkenu double craters (about 95 km west/southwest from J. Arkenu). The impact origin has been confirmed for Oasis and BP (Abate et al. 1997), whereas the Arkenu double craters (Paillou et al. 2003) may eventually need further investigations. The Kebira crater (located on the Libya-Egypt border, about 170 km east/northeast from Kufra) is a 31 km structure identified by satellite imagery and suggested to be a multi-ring impact crater and probably the source of the Libyan desert glass (Boston University Press Release 2006). Two new possible impact structures also have been detected in satellite images in Chad (González and Alonso 2006).

NEW SURVEY

Study Area and Fieldwork

During the fieldwork we visited 7 of the 13 structures identified by Paillou et al. (2004) (GKCF1, GKCF6, GKCF7, GKCF8, GKCF11, GKCF12, and GKCF13) and some others in the surrounding areas (GKS1, GKS2, GKS3) (Figs. 3 and 4). We carried out a detailed geological survey for 5 of these structures (GKCF1, GKCF7, GKCF11, GKCF13, GKS1) where rock samples were also collected for petrographic studies. Geo-electromagnetic field anomalies were measured using the very low frequency (VLF) method at craters GCKF1 and GKCF13. The features of the studied structures are reported in Table 1.

Geology

In the investigated area, the outcropping rocks consist of mostly medium- to coarse-grained, and moderately to poorly sorted quartz-arenites (Fig. 5a) and are characterized by parallel stratification and metric cross-bedding (Fig. 6). They are made up of subrounded/subangular elements of mono- and subordinately polycrystalline quartz and minor lithic grains (likely intraformational, fine-grained quartz-arenites) (Figs. 7 a and 7b). Many quartz grains show an undulose extinction and often micro-fracturing (Fig. 7c). The matrix is made up of very fine-grained quartz grains and phyllosilicates (mainly sericite-illite) (Fig. 7a) and frequently is partially or totally replaced by Fe-Mn oxides/ hydroxides and minor ferriferous carbonates (Figs. 7b and and 7c). Zircon, tourmaline, and muscovite are present as accessory minerals.

Locally micro-conglomerates horizons with rounded/ subrounded mm- to cm-sized quartz grains and lithic fine grained quartz-arenites (Fig. 5b) have been found within the lower part of the arenite-beds.

Intraformational sedimentary breccias (Br1) are also

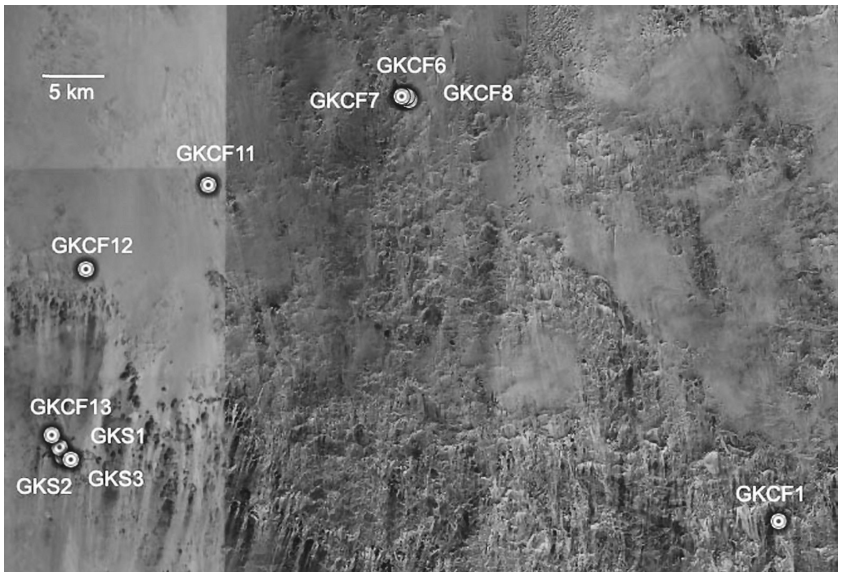

Fig. 3. The investigated structures (view from Google Earth). The latitudes and longitudes are between 23°14′15″–23°34′43″ N and 26°52′10″ –27°31′30″ E, respectively.

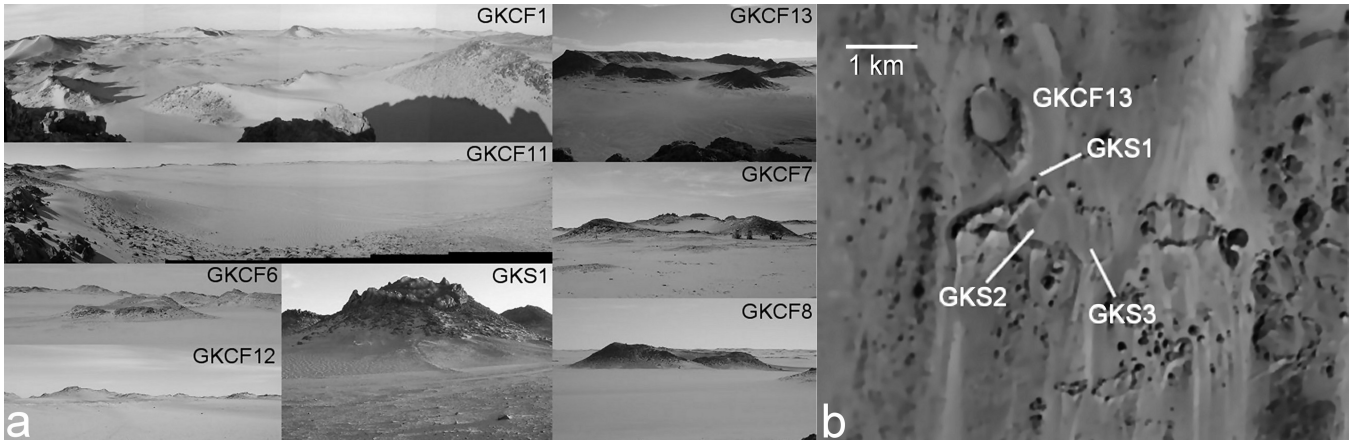

Fig. 4. The investigated structures; their main features are reported in Table 1. a) Panoramic views of some of the investigated craters; GKCF1 (630 m, view to the west), GKCF6 (45 m, view to SE), GKCF7 (75 m, view to N-NW), GKCF8 (90 m, view to SE), GKCF11 (1200 m, view to the south), GKCF12 (500 m, view to SE), GKCF13 (950 m, view to S-SW) and GKS1 (50 m, view to S-SE). b) Quickbird satellite image of GKCF13, GKS1, GKS2 (820 m), and GKS3 (660 m) (spatial resolution 0.6/0.7 m, spectral bandwidth 450–900 nm; from Google Earth).

present as intercalations within the quartz-arenitic succession; they are made by cm- to dm-sized quartz-arenitic clasts, subangular/subrounded in shape (Fig. 5c). The stratigraphic position of these breccias is not always detected but they are often interbedded with the quartz-arenites. Locally they appear to be intensely altered and show dark red or black colors.

A possibly different kind of breccia (Br2) crops out in the rim area of some structures (e.g., GKCF1), both on the inner side and on the outer side (Fig. 8). It consists of angular to subangular, cm- to dm-sized rock fragments (fine- to coarse-grained quartz-arenites and minor siltstones); huge quartz-arenitic laminated boulders (30–40 cm) are also locally present (Fig. 8a). When not altered, the matrix is composed of fine-grained quartz grains and phyllosilicates but often it is totally replaced by iron oxides/hydroxides cement. In this case the breccia shows a dark red or black color for the matrix and a dark yellow color for the clasts. Moreover, boulders of Br1 are included in Br2 in the southern side of GKCF1 (Fig. 8b). The contact between Br2 and the quartz-arenitic lithotypes (visible only in few small outcrops without lateral continuity), appears to be tectonic.

In the surroundings of the crater-like structures, all the above units may be affected by pervasive argillic alteration and often associated with dark brown impregnation horizons of Fe-Mn oxides and sulfides. No basalt dikes have been detected in the studied structures.

The petrographic analysis of quartz-arenites and Br1 and Br2 breccias revealed no characteristic shock deformation features.

The outcropping rocks in the surroundings of these crater-

Table 1.

Id. structure[a]	Geographical coordinates[b] Latitude N	Longitude E	Equivalent diameter (m)	Crater eccentricity	Description and notes[c]
GKCF1	23°14′31″	27°27′32″	650	0.20	Occurrence of breccias (Br1 and Br2) and paleo-soils. Rim partly defined by fracture planes; iron-oxide/hydroxide mineralizations. The nearest volcanic body is at 44.5 km to W-NW (GKCF48).
GKCF6	23°31′45″	27°11′06″	85	0.50	Rim morphology very poorly defined. The nearest volcanic body is at 1.3 km to the north (GKCF50).
GKCF7	23°31′50″	27°10′56″	115	0.30	Rim defined by quartz-arenitic inward dipping layers impregnated by iron-oxide/hydroxide mineralizations. The nearest volcanic body is at 1.2 km to the north (GKCF50). The El-Baz crater is at 110 km to N-NW.
GKCF8	23°31′45″	27°11′16″	160	0.20	Occurrence of sedimentary breccia (Br1). The nearest volcanic body is at 1.3 km to the north (GKCF50).
GKCF11	23°28′15″	27°02′38″	700	0.20	Rim morphology poorly defined. Quartz-arenitic bedrock layers locally impregnated by iron-oxide/hydroxide mineralizations. The nearest volcanic body is at 10.5 km to the south (GKCF48).
GKCF12	23°24′48″	26°57′02″	530	0.00	Rim morphology poorly defined. Occurrence of sedimentary breccia (Br1). The nearest volcanic body is at 11 km to E-SE (GKCF48).
GKCF13	23°18′07″	26°55′33″	850	0.60	Rim defined by quartz-arenitic inward dipping layers impregnated by iron-oxide/hydroxide mineralizations. Occurrence of paleo-soils. The nearest volcanic body is at 10 km to W-NW (GKCF47).
GKS1	23°17′37″	26°55′54″	50	0.40	Rim defined by a mineralized circular fracture plane. The nearest volcanic body is at 9.6 km to the east (GKCF47).
GKS2	23°17′16″	26°56′01″	820	0.35	Occurrence of mineralized fracture/fault planes. The nearest volcanic body is at 9.4 km to E-NE (GKCF47). The Clayton craters are at about 182 km to SW.
GKS3	23°17′07″	26°56′23″	670	0.20	Occurrence of mineralized fracture/fault planes. The nearest volcanic body is at 8.8 km to E-NE (GKCF47).

[a]GKCF1-GKCF13 designate the craters detected by Paillou et al. (2004).
[b]Coordinates refer approximately to the central point of the structures.
[c]GKCF47, GKCF48, and GKCF50 designate structures associated with basalts dikes according to Paillou et al. 2006.

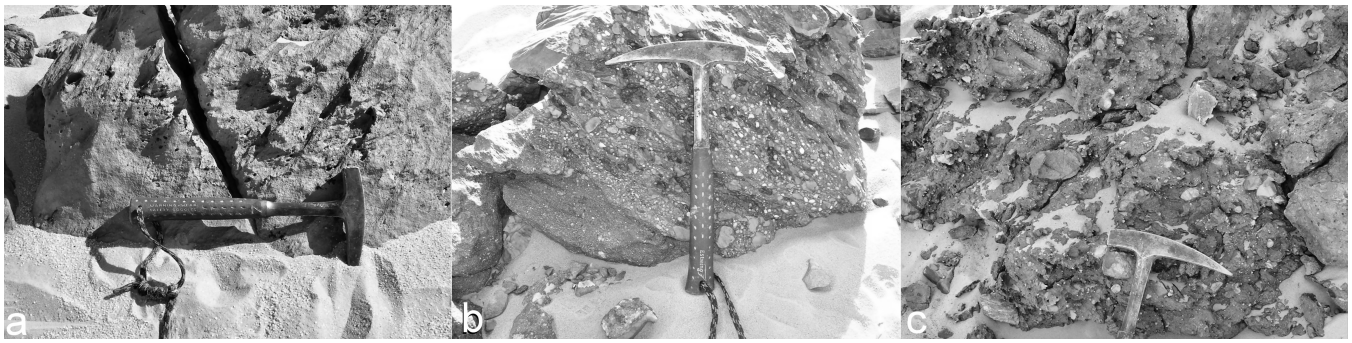

Fig. 5. Bedrock lithologies. a) Quartz-arenites. b) Micro-conglomerate horizon in the lower part of an arenite bed. c) Intraformational sedimentary breccia (Br1), dark red in color.

like structures are characterized by striations (Fig. 9a) that have been possibly interpreted as shatter cones (Paillou 2004, 2006). Shatter cones are conical, striated fracture surfaces that are unequivocally indicative of meteoritic impacts on Earth; they are generally found in rocks located below the crater floor or in the central uplift (if present), but they are also observed within the clasts of the breccia units (French 1998). Our observations show that the striations are not pervasive, superficial features and are not related to fracturing. Moreover, the same striations are visible also onto the surfaces of breccia bodies as well onto the surfaces of the rocks away from the area of the craters (Fig. 9b). These striations, which may be found throughout the region, are characterized by directions that range from 20° to 340° N, which is consistent with main wind directions (from northwest until the early Holocene, from north and northeast at present; Brookes 2003). Thus, it is reasonable to consider these as pseudo-shatter cones derived from the wind abrasion on the exposed rock surfaces.

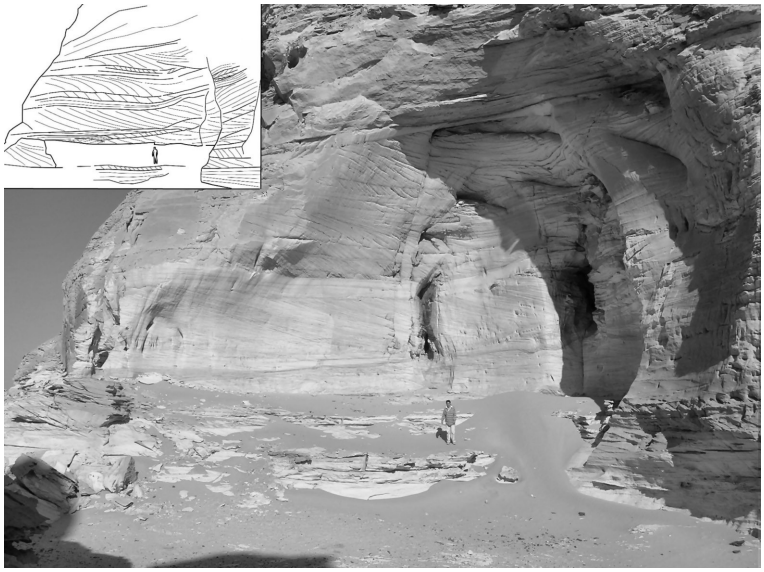

Fig. 6. Megascale cross laminations in the investigated area (Sabaya Formation); in the high left corner the sedimentary surfaces are highlighted.

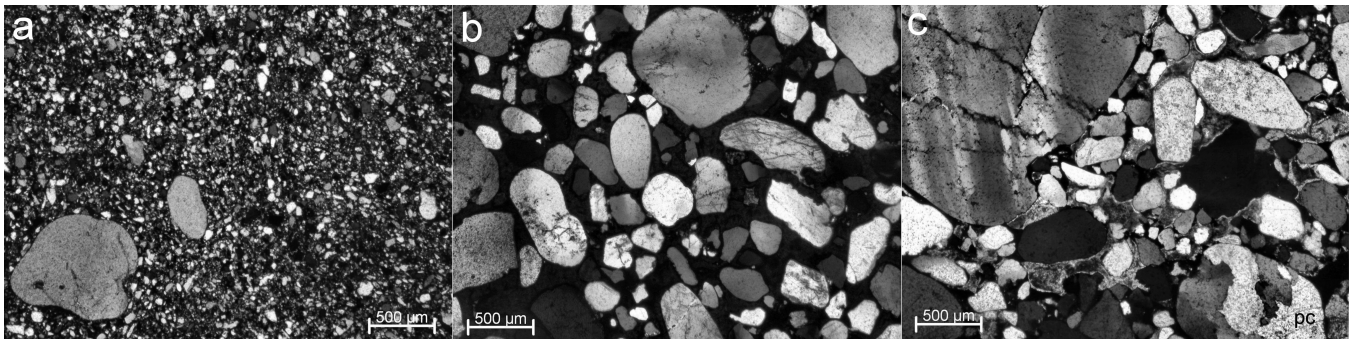

Fig. 7. Microscopic appearance of the quartz-arenites. a) Quartz-arenite composed by subrounded/elements of quartz; the matrix is made up by very fine-grained quartz and phyllosilicates (cross polarized light). b) Quartz-arenite composed by subrounded/subangular elements of quartz; the matrix is totally replaced by Fe-Mn oxides/hydroxides (cross polarized light). c) Poorly sorted quartz-arenite made up of subrounded/subangular elements of mono- and polycrystalline quartz (pc). The matrix is made up by ferriferous carbonates. The quartz element on the left high corner shows undulose extinction and micro-fracturing.

Morphology and Structural Setting

The craters have a roughly circular shape, but in some cases this shape may only be inferred on the basis of satellite images (as in GKCF12 and GKCF6). The rim rises from few meters (as in GKCF7 and GKCF8) to more than 70 m (in GKCF13) above the crater floor (and the surrounding areas). The bottom is always covered by Quaternary aeolian sands and thus the floor is exposed only in the proximity of the inner side of the crater rim. In the investigated structures, the rim is made up of quartz-arenitic beds, exhibiting their typical sedimentary structures, such as parallel- and cross-bedding. These are locally affected by fracturing or fault planes often deeply impregnated by oxide/hydroxide mineralizations, and consequently highlighted by the selective erosion. In particular, in some of the investigated structures (e.g., GKCF13 and GKCF7) the rim consists of quartz-arenitic inward dipping layers, with rare evidence of fracturing (Fig. 10). They are not tilted as a result of the "impact crater" formation as previously suggested (Paillou et al. 2004, 2006), but they show the original setting, related to megascale cross laminations that are typical of the bedrock in this area (Fig. 6). This observation is also supported by the presence of nearly horizontal quartz-arenitic layers in some rim areas and by the fact that many "tilted" layers extend also out of the craters rim. Thus, these evidences do not support an impact origin.

In other key cases, the rim is defined by linear or arc-shaped nearly vertical fracture planes (Fig. 11) such as in GKCF1 and GKS1. The arcuate fracture planes affect not only the rim of craters-like structures, but they are detectable also in their periphery. The linear fracture planes are oriented N-S, NE-SW, and NW-SE, they are internal and external to the circular structures and possibly predate the arcuate fracture planes. The intersection of these two sets of fractures often

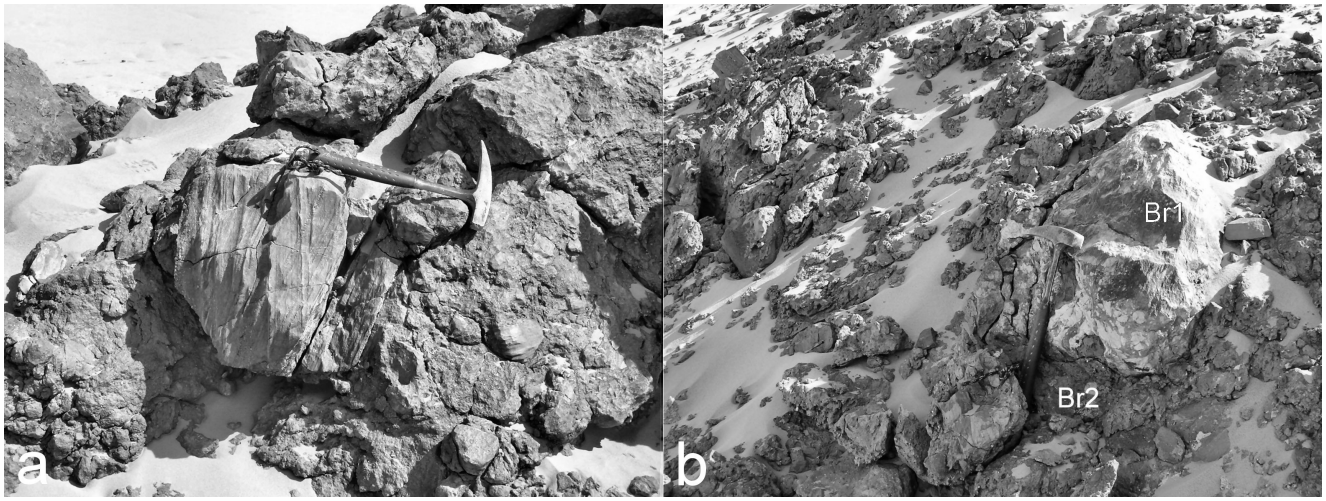

Fig. 8. Br2 breccia from GKCF1. a) Decimetric quartz-arenitic laminated boulder included in Br2 breccia. b) Br1 boulder included in Br2 breccia.

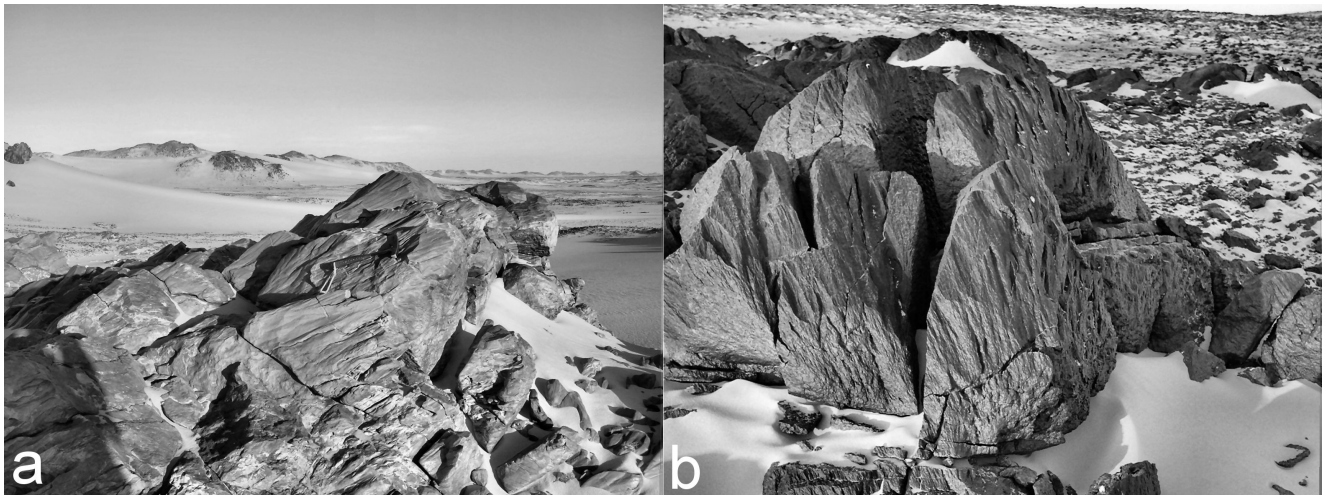

Fig. 9. Shatter cones-like features. a) Striations on quartz-arenites at GKCF13. b) Striations on basalts at El-Baz volcanic crater.

Fig. 10. Rim defined by oblique sandstone layers. a) GKCF13 (view to the west), the crater floor is on the left; an angular unconformity is visible in the rectangle. b) GKCF7 (view to NW), the crater floor is on the right.

Fig. 11. Crater rim defined by fracture planes. a) Arc-shaped fracture plane in GKCF1 (view to the west). b) Linear fracture plane in GKCF1 (view to NW). c) Anular fracture plane in GKS1 (view to S-SE).

affects the rim shape. Fe-Mn oxide/hydroxide mineralizations are associated with the fracture zones and this is observable not only at the "crater-scale," but also at smaller scale (e.g., cm-sized fractures on the craters floor). Moreover, the fracture planes are frequently associated with Br2 breccia bodies.

Geophysical Survey

A geophysical survey was carried out to define the subsurface setting of the GKCF1 and GKCF13 structures using the very low frequency electromagnetic (VLF-EM) technique. This is a passive electromagnetic prospecting method that works within a low frequency range (15–30 KHz) (e.g., Reynolds 1997), and yields geo-electromagnetic field (GEF) anomalies.

VLF-EM transmitters are located at several points around the world and broadcast at frequencies of 15–25 kHz. The VLF-EM systems make use of the energy of these distant radio transmitters as a fixed transmitter array, and obtain the geo-electromagnetic field (GEF) anomalies, thus measuring the real and imaginary components of the "secondary field" as a percentage of the "primary field."

Impact craters are generally associated with a circular distribution of the GEF anomalies due to the bowl-shaped morphology of the inner part and the thickness of the infilling deposits that decrease from the centre to the margins. The in-phase and quadrature measurements in 2-D contour maps can locate the position of the GEF anomalies and single profile peaks reveal the subsurface structures.

In our survey we used Abem Wadi Instrumentation (Abem Instrument AB 1993), that is compact and easily transportable. In the investigated areas we recorded distinct electromagnetic anomalies, likely due to Fe-Mn oxide/hydroxide impregnations present within fractures and faults located in the basement rocks. For this reason, we considered the probable superimposition of these anomalies with those due to the thickness of the infilling deposits.

GKCF1: The softly undulated to flat morphology of the site allowed us to carry out a survey along 18 60° N-trending profiles spaced 20 m apart. The maximum length of the profiles were roughly coincident with the diameter of the structure. The differences in elevation of the single-spot measurements did not play a significant role in generating the shape of the anomalies, since their scale is small in respect to the variations of the horizontal distances among single spots. We used GPS for constructing the inner topography of the circular structure and to georeference the single stations on the map. The collected data show that the main GEF variations measured at GKCF1 (Fig. 12) have a different trend from the expected ones typical of impact craters and suggest a widespread and small thickness of the infilling deposits. The GEF variations do not show a circular

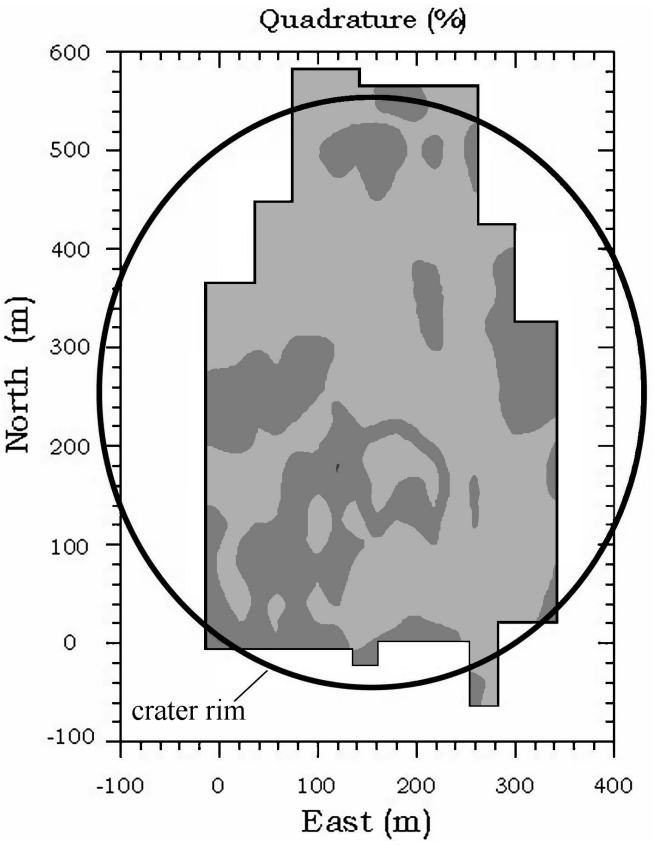

Fig. 12. Distribution of the GEF values anomalies in the GKCF1; the circle indicates the rim of the structure. The higher values (dark grey) are associated to Fe-Mn oxide/hydroxide mineralizations pervading the rocks cropping out in the rim or to the thickness variations of the infilling sands.

distribution. The higher values (–40% to +80%) follow a N-S linear distribution, locally aligned to the main mineralized fracture planes cutting the bedrock cropping out on the ridges around the circular structure. No meaningful variation of GEF values are present near the rare bedrock outcrops observed inside the crater.

GKCF13: The surface of the crater floor in GKCF13 is regular and gently tilted to southwest. It is made up of rocky debris overlain by thin aeolian sands. No rocky materials are present far away from the relieves of the crater rim. At GKCF13 we carried out a GEF survey along 5 profiles, placed 30 m apart thus covering nearly half of the central crater area. The application of GPS techniques allowed us to deploy a network for systematic measurements as well as to outline the topography of the area. In this case, we did not record significant variations of the GEF, and only few minor and isolated anomalies were decoded (max. 20%). They could be related to the presence of large boulders buried underground or, alternatively, to a different thickness of the infilling deposits. The combination of GEF and field data indicates that the infilling deposits have a maximum thickness of at least 30 m and mineralized fractures and faults are rare when compared to the GKCF1 site.

The reconstructed subsurface morphology of both sites investigated suggest that they have not a bowl shape.

DISCUSSION

Paillou et al. (2004, 2006) suggested that the Gilf Kebir crater field could be the result of meteoritic impacts. Here we review such hypothesis by taking into account the new data collected during our campaign.

Arguments in Conflict with the Impact Hypothesis

Microscopic Effects of Shock Metamorphism

The target rocks do not show any microscopic shock effects, in particular no planar deformation features (PDFs), no evidence of melting and/or presence of glass. However, it is worth to note that in porous sedimentary target the shock effects are not always well developed and impacts produce distinct effects from those involving non-porous crystalline targets (Grieve et al. 1996). In fact, on the basis of the observations of shock effects on the Coconino Sandstones at Meteor Crater (Arizona), it is possible to see a progressive obliteration of the original texture: at the lowest pressure (<5 GPa) the porosity is reduced to zero and the minerals are fractured; at moderate pressure (5–13 GPa) fractured quartz coexists with minor amounts of glass and coesite (French 1998). In the Gilf Kebir, there are no apparent differences between rocks inside and outside the craters. Their porosity is still well preserved, the quartz grains are only rarely deformed and glass is absent.

We found no evidences for the shocked quartz formerly described by Paillou et al. (2004, 2006) in sandstones and breccias of this area. Deformation features found in quartz grains of the sampled rocks do not have any similarities with PDFs in impactites and are the result of "normal" tectonic processes. However, PDFs in porous targets, compared to non-porous rocks, are generally rare (Grieve et al. 1996).

In addition, shocked quartz grains occur not only in parautochthonous target rocks of the crater floor, or in allochthonous lithologies, such as breccias or impact melt rocks, but also in various types of proximal and distal ejecta. The presence of rare and isolated shocked quartz grains in a clastic sedimentary rock (without additional impact evidences) can be virtually the result of the erosion of a distant impact structure.

Macroscopic Effects of Shock Metamorphism

The presence of shatter cones is considered an unequivocal fingerprint of meteoritic impacts on Earth, but other structures have similar morphology, for example natural percussion marks, slickensides, wind abrasion structures and cone-in-cone structures. The axes of shatter cones are generally described as pointing toward the shock waves source area but many cases of non-radial orientation are known (Baratoux and Melosh 2003). Our data suggest that the observed structures are superficial features characterized by a narrow strike range, thus supporting the idea that these shatter cone-like features are instead originated by the effect of wind erosion. Moreover, the same striations are visible also onto the surfaces of the breccia bodies, involving both the clasts and the matrix: this evidence clearly is in contrast with the "authenticity" of the shatter cones or with an impact origin of the breccia itself. Finally, no other macroscopic impact indicators were identified.

Impact Lithologies

Impact breccia has been tentatively identified by Paillou et al. (2004). During our survey, we found two kinds of breccias: a sedimentary intraformational breccia (hereby named Br1) and Br2, which has a more complex setting, generally discordant with the bedrock structures, and, conversely, concordant with the fracture planes located at the crater's rim. Therefore, Br2 is genetically linked to the origin of the circular structures (see further discussion). Nevertheless, both breccias do not show any microscopic shock effects or shock minerals and no evidence of glass or melting were observed in these rocks.

It is worthy to note that some impact breccias are melt-free and with distinctive shock effects only rarely observed in the fragments ("impact lithic breccias"). This kind of breccia is often associated, horizontally and/or vertically, with units containing melts or shocked minerals and so the exact identification of the lithic breccia is possible. These associations are not evident for Br2 and, therefore, it cannot be interpreted as related to an impact.

Circular Morphology

The circular shape of several structures noticed in the area by Paillou et al. (2004, 2006), both in the field and satellite imagery, was ascribed to meteoritic impacts. According to this view, these structures would be part of an impressive crater field made by thousands of craters spread over thousands of km^2 (nothing similar has been identified so far on the Earth). Some of these structures are also associated with basalts (as 5 of the 62 craters identified by Paillou et al. 2006, see Table 1 for the distances with respect to the studied structures). Moreover, the geophysical survey suggests that they do not show the bowl shape typical of impact craters. Morphological similarities between the 10 investigated structures and many others structures in the surroundings (together with the absence of clear impact evidences and relict meteoritic materials) lead us to regard all these features as geological structures.

Therefore our investigations do not support the impact hypothesis for the origin of the Gilf Kebir structures.

Hydrothermal Venting: A More Plausible Hypothesis

The presence of such an extended field of circular structures, linked to a widespread volcanic activity in the surroundings and to the evidence of an intense fluid circulation in the craters area, localized in particular along the fracture planes, suggest a possible hydrothermal origin for these structures (one of the hypotheses indicated also by Paillou et al. 2006). Hydrothermal venting may be a plausible explanation for the origin of such an extended field of nearly circular features—what we actually see could be the result of the erosion of a former hydrothermal field likely underlain by subvolcanic intrusives and/or minor igneous plugs and unvented dykes.

In some of the studied structures, the arcuate fracture planes seem to be strictly connected to the crater-like forms. They define the rims, partly as in GCKF1, or totally as in GKS1; concentric fracture planes are also present in the immediate periphery of the cited structures, visible also in satellite imagery. The origin of the arcuate fractures and ring-faults in the studied region could be related both to the increase of fluids pressure in the initial phase of magma chambers development and to the subsequent gravitational sliding during their collapse (Folch and Marti 2004). The interaction between the arcuate fracture set and the linear fracture set (possibly pre-existing) define the shape of the pseudo-craters. The quartz-arenitic bedrock in these structures has a general horizontal setting.

In other cases the crater rim is not delimited by fracture planes (as in GKCF13 and 7), but by quartz-arenitic gently dipping mineralized beds and cross-beddings that, as previously exposed, represent the original pre-crater formation setting. In this case, the absence of arcuate fracture planes could be related simply to the bedrock setting—the dipping layers likely favoured and increased fluid migration, reducing the effect of local over-pressures that, in turn, would have developed extensive fracturing. The situation at GCKF1, where no dipping layers are present, support this hypothesis—the rim is defined in fact by arcuate and linear fracture planes.

Within a hydrothermal model the brecciation could be locally fluid-induced and related to pore pressure fluctuations. These hydrothermal fluids were enriched in iron oxides inherited from interaction with oxidized sediments or paleo-soils. The pre-existing sets of fracture planes and sedimentary structures could have controlled the circulation of fluids and contributed to the origin of the current structural pattern.

CONCLUSIONS

On the basis of our fieldwork and investigations, we can state that there are no evidences supporting the impact origin of the circular structures in Gilf Kebir region. The alternative hypothesis hereby suggested may also apply to other structures in the near field, but it cannot be excluded that some genuine impact structures may exist in the whole region.

In the light of the above, we emphasize that some other circular structures of the Sahara region, detected from satellite images and previously interpreted as impact craters, could also have a different origin and should be further investigated. The peculiar geological setting of the cratonic Sahara region, which includes several volcanic units and structures that cross-cut thick porous quartz-arenitic successions, together with the occurrence of selective and persisting erosion can lead to the formation of circular structures that may resemble impact craters.

In a similar fashion, the structure of el-Mrayer (Mauritania), detected using ASTER image (Rossi 2002) and investigated in 2002 by one of us (M. Morelli), shows strong geological and morphological similarities with the structures in the Gilf Kebir area. In this site, the Precambrian crystalline basement is overlain by a thick succession of porous sandstones cut by a tight network of fractures and fault planes that show abundant Fe-Mn oxide/hydroxide mineralizations. As in the Gilf Kebir region, selective erosion clearly exposed the mineralized fractures and preserved linear to arcuate ridges with a moderate elevation with respect to the surrounding areas. The ridges are made by mineralized sandstones and breccias. Pseudo-shatter cones are also present, and no evidence of impact related rocks was found.

In conclusion, the data collected during our fieldwork support the hypothesis that the circular structures detected in the Gilf Kebir area are related to endogenic geological processes typical of volcanic areas, such as extended geothermal fields that have been activated after the deposition of a sedimentary cover. These cover units have been partly affected by fluid migration that locally produced argillic alteration and Fe-oxide/hydroxide and sulfide impregnations before, during and after hydrothermal

venting. This process seems to be related to the emplacement of subvolcanic igneous plugs and dykes that did not reach the surface and crystallized at depth undergoing degassing.

Acknowledgments—We are grateful to Vincenzo de Michele for the discussions and suggestions, and to Luca Matassoni of Prato Ricerche Fundation and Romano Serra of Department of Physics of Bologna University for their help in the field survey. We are also grateful to Shereef Shousha and Ali Barakat (Egyptian Geological Survey and Mining Authority), and Maria Casini (Italian Embassy in Cairo) for their support in organizing the field expedition, and to Gabriella Losito (University of Florence) for providing the VLF instrumentation. Benito Piacenza, who recently with our deepest sorrow left us, and Degussa Novara Technology S.p.A. for the excellent thin sections they provided. The constructive reports of the two referees, B. M. French and F. de Souza, are also kindly acknowledged.

Editorial Handling—Dr. John Spray

REFERENCES

Abate B., Koeberl C., Underwood J. R., Reimold W. U., Buchanan P., Fisk E. P., and Giegengack R. F. 1997. BP and Oasis impact structures, Libya: preliminary petrographic and geochemical studies, and relation to Libyan desert glass (abstract). 28th Lunar and Planetary Science Conference. pp. 1–2.

Abdelsalam M. G., Liégeois J-P., and Stern R. J. 2002. The Saharan Metacraton. *Journal of African Earth Science* 34:119–136.

Abem Instrument AB. 1993. *ABEM interpretation guide—ABEM Wadi VLF Instruments*. 36 p.

Barakat A. 1994. El-Baz crater: Basaltic intrusion versus meteoritic impact crater. *Annals of Geological Survey of Egypt* 24:167–177.

Baratoux D. and Melosh H. J. 2003. The formation of shatter cones by shock wave interference during impacting. *Earth and Planetary Science Letters* 216:43–54.

Brookes I. A. 2003. Geomorphic indicators of Holocene winds in Egypt's Western Desert. *Geomorphology* 56:155–166.

Clayton P. A. 1933. The western side of the Gilf Kebir. *Geographical Journal* 81:254–259.

Dardir A. A. 1982. Basement rocks of the Gilf-Uweinat area. In *Desert landforms of southwest Egypt: A basis for comparison with Mars*, edited by El-Baz F. and Maxwell T. A. Washington D.C.: National Air and Space Museum. pp. 67–78.

El-Baz F. 1981. The "Uweinat Desert" of Egypt, Libya and Sudan: A fertile field for planetary comparisons of crater forms (abstract). 12th Lunar and Planetary Science Conference. pp. 251–253.

El-Baz F. and Issawi B. 1982. Crater forms in the Uweinat region. In *Desert landforms of southwest Egypt: A basis for comparison with Mars*, edited by El-Baz F. and Maxwell T. A. Washington DC: National Air and Space Museum. pp. 79–89.

Boston University Press Release. 2006. Largest crater in the great Sahara discovered by Boston University scientists. http://www.bu.edu/phpbin/news/releases/display.php?id=1073.

French B. M. 1998. *Traces of catastrophe: A handbook of shock-metamorphic effects in terrestrial meteorite impact structures*. Houston, Texas: Lunar and Planetary Institute. 120 p.

Folch A. and Marti J. 2004. Geometrical and mechanical constraints on the formation of ring-fault calderas. *Earth and Planetary Science Letters* 221:215–225.

French B. M., Underwood J. R., and Fisk E. P. 1974. Shock metamorphism features in two meteorite impact structures, south-eastern Libya. *Bulletin of Geological Society of America* 85:1425–1428.

González E. and Alonso S. 2006. Evidence of two new possible impact structures in Chad: Separate impacts, binary asteroids or Aorounga impact chain? (abstract). Proceedings, Workshop on Impact Craters as Indicators for Planetary Environmental Evolution and Astrobiology. CD-ROM.

Grieve R. A. F., Langenhorst F., and Stöffler D. 1996. Shock metamorphism of quartz in nature and experiment: II. Significance in geoscience. *Meteoritics & Planetary Science* 31:6–35.

Issawi B. 1982. Geology of the southwestern desert of Egypt. In *Desert landforms of southwest Egypt: A basis for comparison with Mars*, edited by El-Baz F. and Maxwell T. A. Washington D.C.: National Air and Space Museum. pp 57–66.

Klitzsch E., List F. K., and Pöhlmann G. 1987. *Geologic Map of Egypt 1:500.000*. Cairo, Egypt: The Egyptian General Petroleum Corporation. 20 sheets.

Koeberl C. and Reimold W. U. 2002. Field studies at the BP and Oasis impact structures, Libya (abstract). *Meteoritics & Planetary Science* 37:A79.

Koeberl C., Reimold W. U., Vincent P. M., and Brandt D. 1998. Aorounga and Gweni Fada impact structures, Chad, Central Africa: Petrology and geochemistry of target rocks (abstract #1103). 29th Lunar and Planetary Science Conference.

Koeberl C., Reimold W. U., Cooper G., Cowan D., and Vincent P. M. 2005. Aorounga and Gweni Fada impact structures, Chad: remote sensing, petrography, and geochemistry of target rocks. *Meteoritics & Planetary Science* 40:1455–1471.

Paillou Ph., Rosenqvist A., Malezieux J. M., Reynard B., Farr T., and Heggy E. 2003. Discovery of a double impact crater in Libya: The astrobleme of Arkenu. *Comptes Rendus Géoscience de l'Académie des Sciences* 335:1059–1069.

Paillou Ph., El-Barkooky A., Barakat A., Malezieux J. M., Reynard B., Dejax J., and Heggy E. 2004. Discovery of the largest impact crater field on Earth in the Gilf Kebir region, Egypt. *Comptes Rendus Géoscience de l'Académie des Sciences* 336:1491–1500.

Paillou Ph., Reynard B., Malezieux J. M., Dejax J., Heggy E., Rochette P., Reimold W. U., Michel P., Baratoux D., Razin Ph., and Colin J. P. 2006. An extended field of crater-shaped structures in the Gilf Kebir region, Egypt: Observations and hypotheses about their origin. *Journal of African Earth Science* 46:281–299.

Peel R. F. 1939. The Gilf Kebir. *Geographical Journal* 93:295–307.

Reynolds J. M. 1997. *An introduction to applied and environmental geophysics*. New York: Wiley & Sons. 796 p.

Rossi A. P. 2002. Seven possible new impact structures in Western Africa detected on ASTER imagery (abstract #1309). 33rd Lunar and Planetary Science Conference. CD-ROM.

Said R. 1990. *The geology of Egypt*. Rotterdam, Netherlands: A. A. Balkema Publishers. 734 p.

Schlüter T. 2006. *Geological atlas of Africa*. Berlin, Heidelberg, New York: Springer-Verlag. 272 p.